Available online at www.sciencedirect.com

ScienceDirect

Ceramics International 38 (2012) 373–379

CERAMICS INTERNATIONAL

www.elsevier.com/locate/ceramint

Synthesis of ultradisperse $NiFe_2O_4$ spinel by thermal decomposition of citrate precursors and its magnetic properties

T. Karpova [a,*], V. Vassiliev [a], E. Vladimirova [a], V. Osotov [b], M. Ronkin [b], A. Nosov [b]

[a] Institute of Solid State Chemistry, Ural Division of RAS, 91 Pervomaiskaya Str., GSP-170, Ekaterinburg 620041 Russia
[b] Institute of Metal Physics, Ural Division of RAS, 18 S. Kovalevskaya Str., GSP-170, Ekaterinburg 620041 Russia

Received 12 April 2011; received in revised form 6 July 2011; accepted 8 July 2011
Available online 2nd August 2011

Abstract

Peculiarities of synthesis of nanocrystalline $NiFe_2O_4$ powders by thermal decomposition of citrate precursors were investigated. It was found that the parameters of nanopowders are determined by the decomposition temperature and pH of the precursor media. The temperature and duration of the process of precursor decomposition are limiting factors for decrease of the grain size. An optimum relation between the limiting factors can be determined experimentally by variation of pH. Correlation between the synthesis parameters, particle size, and magnetic properties is discussed. It is shown that optimum magnetic and magnetostrictive properties were found for the bulk polycrystalline samples sintered using the powders obtained for pH 2.

Keywords: A. Powders: chemical preparations; D. Ferrites; D. Spinel; C. Magnetic properties

1. Introduction

The spinel ferrites of general formula MFe_2O_4, where M = Mn, Co, Ni, Zn, attract considerable interest as soft magnetic materials for potential applications in magnetic field sensing, ferrofluids, magnetic drug delivery, magnetic information storage, and high frequency devices. The advantage of these materials is in high magnetostriction and high rate of change of strain with magnetic field [1]. In recent years the evolution of physical properties of materials upon transition from macroscopic bulk state to the nanocrystalline one have been intensively investigated. This transition is accompanied by substantial changes of electronic structure: the continuous density of states is replaced by set of discrete levels the exact position of which is determined by a particle size [2]. With decreasing a particle size the fraction of surface atoms with smaller coordination number, broken chemical bonds, and disrupted local symmetry, also increases. Owing to these reasons not only the properties of surface atoms differ substantially from those of atoms in a particle core, but also the character of interactions between these groups of atoms can have additional peculiarities. All these factors result in appearance of principally new physical properties of nanocrystalline state as compared to the bulk one.

For the spinel ferrites in ultradisperse and nanocrystalline states the cation distribution, and degree of inversion can differ from the corresponding bulk values which results in variation of magnetic and magnetoelastic properties. Strong dependence on preparation method [3,4], thermal treatment conditions [1], particle size [5], and morphology [6,7] was observed.

Various methods have been developed for preparation of ultradisperse and nanocrystalline powders of spinel ferrites, namely the sol–gel [8,9], hydrothermal synthesis [10,11], organic complexes, combustion processes with various precursors [12–15]. The possibility of formation of ultradisperse Fe-based complex oxides by thermal decomposition of citrate precursors was demonstrated in [15–17]. The advantage of this method is in the fact that the gaseous products, which are formed during the process of thermal decomposition of complex compounds, can hinder formation the large sized particles of complex oxides [18]. The authors of [19] describe the method of synthesis of $NiFe_2O_4$ fibers with certain dimensions upon variation of pH, namely by regulation the conditions of formation of an organic complex.

---

* Corresponding author.
E-mail address: Geoma2006@yandex.ru (T. Karpova).

0272-8842/$36.00 © 2011 Elsevier Ltd and Techna Group S.r.l. All rights reserved.
doi:10.1016/j.ceramint.2011.07.016

In this work we report the peculiarities of synthesis of ultra- and nanosized spinel nickel ferrite $NiFe_2O_4$ using the method of decomposition of citrate precursor. The magnetic and magnetostrictive properties of thus obtained samples were investigated.

2. Experimental details

2.1. Sample preparation

The method of decomposition of citrate complex of corresponding metals was used for synthesis of the $NiFe_2O_4$ spinel ferrite. The high purity Fe, NiO, $C_6H_8O_7$, HNO_3 in proportion of $M(Ni):M(Fe):M(C_6H_8O_7) = 1:2:2.7$ were taken as initial reagents. Such relation between the components has been taken with an account for the condition of equilibrium of oxidation-reducing reaction. The $C_6H_8O_7$ have been taken with $\sim$20% excess. The detailed synthesis chart is shown in Fig. 1. To obtain the citrate complex, the $Ni(NO_3)_2{\cdot}6H_2O$ and $Fe(NO_3)_3{\cdot}9H_2O$ aqueous solutions were prepared first by dissolution of Fe and NiO with $\approx$30% excess of HNO_3. Thus obtained solutions were mixed and the required quantity of aqueous solution of citric acid was added under permanent stirring. As the result of such process the organic complexes were formed. The resulting solution was divided into three portions to which the NH_4OH solution was added by droplets. In these portions the pH value of solution was 2, 7, 11. The corresponding samples were named as No. 1, No. 2, and No. 3. The solutions were evaporated at 95–100 °C for 2–3 h till formation of gels. The temperature in the reaction zone was controlled with 1 s interval using the Pt/Pt–10Rh thermocouple. The pH of reacting media was kept at constant value by droplet addition of NH_4OH solution. Subsequent heating resulted in combustion of gels and formation of dispersed precursors. Thus obtained precursors were carefully grinded and annealed gradually increasing the temperature from 350 to 900 °C until the single phase polycrystalline $NiFe_2O_4$ powder was obtained.

2.2. Characterization

The phase composition of the samples was analyzed using the Shimadzu XRD-7000 diffractometer (monochromatic Cu Kα radiation with $\lambda = 0.15418$ nm) at room temperature. Diffraction spectra were recorded with the speed of 0.9°/min in the interval of 2θ from 20° to 80°. For phase identification the data of the JCPDSD-ICDD card No. 00-054-0964 were used. The structural parameters were determined using the FullProf Suite (Version: 2.00) software. Surface topography and composition of the sintered samples were investigated using the JEOL JSM-6390LA secondary electron microscope with energy dispersive analyzer. For proper determination of the nanocrystallite dimensions and size distributions images from more than 10 areas from each sample were treated.

The infrared (IR) absorption spectra were recorded using the IR Fourier spectrometer ‘‘Vertex 80’’ (Bruker) in the spectral range from 4000 to 400 cm^{-1}. The powder samples with admixture of CsI were used.

For magnetic measurements the powders were isostatically pressed under the pressure of $P = 150$ kgf/cm^2 and the pellet-shaped samples with the diameter of 10 mm and thickness of

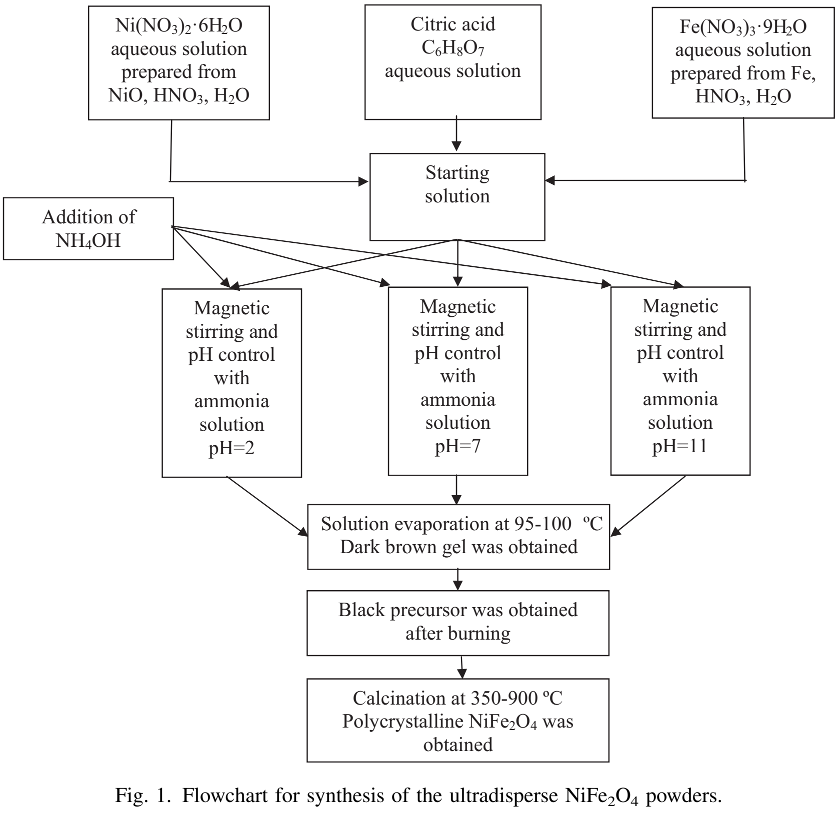

Fig. 1. Flowchart for synthesis of the ultradisperse $NiFe_2O_4$ powders.

1 mm were obtained. The pellets were thermal treated in air at 900 °C for 6 h. Static magnetic measurements were made using vibrating sample magnetometer. Magnetostriction was measured at room temperature in the direction parallel to the applied field using resistive strain gauges glued to the samples. Magnetization curves were recorded using the Quantum Design SQUID magnetometer and Cryogen Free Mini VSM Measurement System.

3. Results and discussion

It is known that the citric acid forms the complex compounds with metal ions, such as Fe^{3+} and Ni^{2+}. As the result of mixing the solutions of iron and nickel nitrates with HNO_3 excess and the solution of citric acid the chemical composition of the final product – $NiFe_2O_4$ – is formed which exists at this stage in the form of sol – the high disperse colloidal solution. In course of evaporation at the temperatures 95–100 °C an abrupt increase in concentration of dispersed phase occurs. This results in appearance of contacts between particles and beginning of gel formation. Analysis of IR spectra of the samples Nos. 1–3 showed that the organic complexes have similar structure. The most probable structure of the complex is shown in Fig. 2. Detailed analysis of the IR spectra will be reported in a separate publication. With the addition of aqueous HNO_3 solution the structure of complex remains unchanged, however, chemical interaction between NH_4OH and excess of HNO_3 takes place according to the standard scheme

$$NH_4OH + HNO_3 = NH_4NO_3 + H_2O \tag{1}$$

Thus, HNO_3 remains in excess in the sample No. 1, the neutralization reaction with formation of NH_4NO_3 and H_2O takes place in the sample No. 2, and the same reaction occurs in the sample No. 3 though an excess of NH_4OH appears. Subsequent heating of gels Nos. 1–3 at 100–130 °C results in decomposition of the citrate precursors obtained. The fast reaction of decomposition of citrate complex, being accompanied by decomposition of ammonium nitrate, is characterized by strong exothermic effect and appearance of naked flame. The ammonium nitrate plays the role of detonator in the process of burning. In the sample No. 3 an excess of ammonium hydroxide is present alongside with the ammonium nitrate. The results of numerous experiments showed that, since the addition of aqueous solution of ammonia does not influence the structure of the complex, it is reasonable to make the pH measurements of the reacting media at the final stage of evaporation of water from solution.

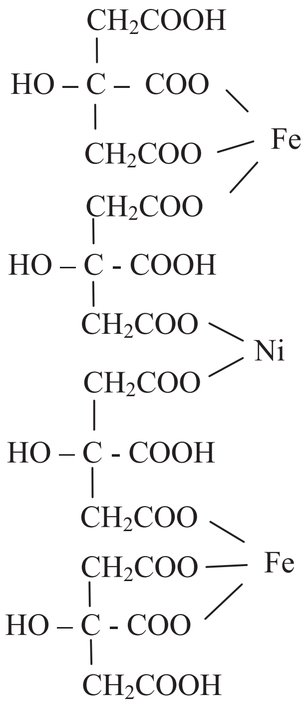

Fig. 2. Proposed structure of the citrate precursor for synthesis of $NiFe_2O_4$.

Thermal decomposition of NH_4NO_3 can occur in blusterous way and is accompanied by inflammation. Two reactions are possible

$$NH_4NO_3 \rightarrow NOx + 2H_2O \tag{2}$$

$$2NH_4NO_3 = 2N_2 + O_2 + 4H_2O \tag{3}$$

The reaction (2) flows at temepratures below 250 °C, while the reaction (3) – at temperatures above 300 °C in the presence of detonator or organic acids. In the case of decomposition of citrate precursors the explosibility of ammonium nitrate increases substantially owing to an abrupt decrease of water content upon gel heating and availability of the citrate complex of nickel and iron which is the component with high calorific value. In the gel No. 3 NH_3 is also present.

Variation of temperature in course of thermal decomposition of the citrate precursor is shown in Fig. 3(a)–(c) for the samples Nos. 1–3, respectively. It is seen that the process of burning occurs in different ways depending on the pH values: in the acid medium the temperature of burning does not exceed 228–230 °C and the process is rather long (about 230 s), while in the neutral medium the temperature of burning is maximum and is equal to 460 °C. In this case the rate of temperature increase upon ignition is about 140 °C/s but then the temperature decays slowly, though in the whole the process occurs faster than in the case of sample No. 1 and lasts about 125–130 s. In the alkaline medium the temperature of burning is equal to 420 °C, the process occurs very quickly (less than in 40 s), and the rate of temperature increase upon ignition is about 65 °C/s. Probably the process of detonation of NH_4NO_3 in a neutral medium is more intensive, however, the duration of the burning process decreases upon transition of the medium of citrate precursor from acid to the alkaline one.

After thermal decomposition of gels the amorphous precursors were obtained which were subsequently thermal treated at temperatures from 300 to 900 °C in air. Since the X-ray diffraction patterns of all samples differed only slightly, only the data for sample No. 2 are shown in Fig. 4. It is seen that at temperatures of thermal treatment below 900 °C the peaks of both the final product – $NiFe_2O_4$ and the Fe_2O_3 impurity are seen. The diffraction pattern for the sample treated at 900 °C contains only the peaks of the final product. This suggests that

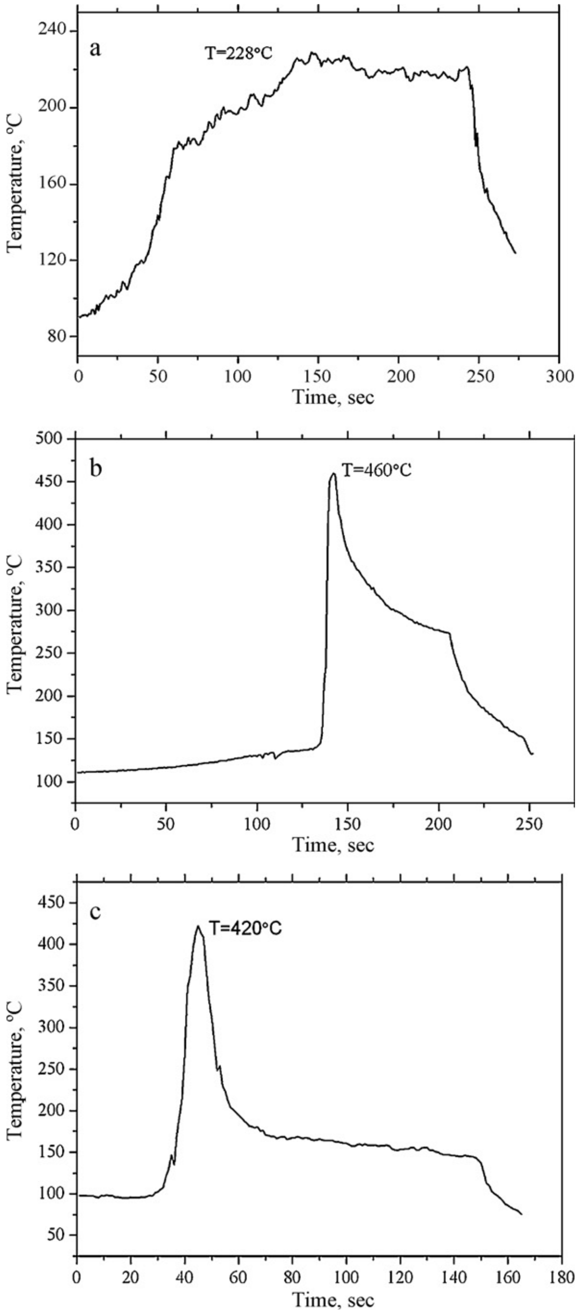

Fig. 3. Variation of temperature during the process of thermal decomposition of gel: (a) for the sample No. 1 with pH 2, (b) for the sample No. 2 with pH 7, (c) for the sample No. 3 with pH 11.

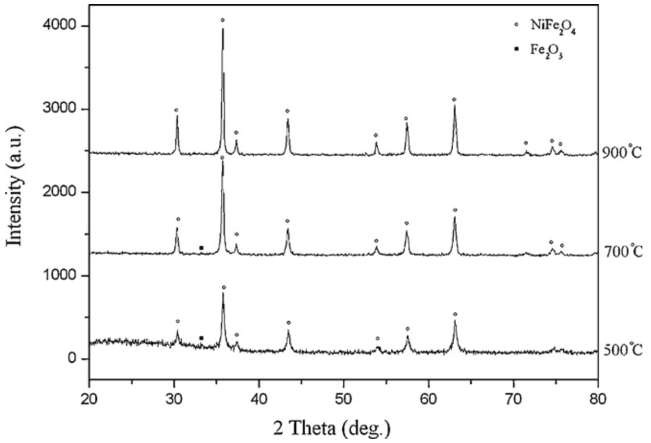

Fig. 4. The X-ray diffraction pattern for the $NiFe_2O_4$ sample No. 2 with pH 7 obtained by thermal decomposition of the citrate precursor with subsequent thermal treatment at temperatures 500–900 °C.

upon decomposition of amorphous precursor a spinel ferrite is formed with defects and oxygen nonstoichiometry. Upon subsequent temperature increase, the crystalline structure is stabilized and the $NiFe_2O_4$ powder with better stoichiometry and homogeneity is formed.

The spinel ferrite $NiFe_2O_4$ has the cubic symmetry (the space group $Fd{-}3m$). The lattice parameters determined from the X-ray spectra are given in Table 1. The relative error of determination of cell volume does not exceed 0,5%. The values of lattice parameters obtained are in good accordance with the known literature data for polycrystalline $NiFe_2O_4$ [20].

The SEM images of the surface topography for the samples investigated are shown in Fig. 5(a)–(c) for the samples Nos. 1–3, respectively. It is seen that the polycrystalline samples consist from particles with typical dimensions 50–120 nm which are randomly distributed and form granules of greater dimensions. The granules form large agglomerations. The dimensions of such agglomerations can vary from ~150 nm till units of micrometers. Note that the grain size increases with temperature and the presented data correspond to the samples obtained after thermal treatment at 900 °C (see Table 2).

Fig. 6(a)–(c) shows the particle size distributions obtained by treatment of the SEM images. An average particle size, its absolute and relative errors were determined implying the standard Student's distribution. The values of the absolute and ratio errors are minimal for the sample No. 2 which correlates with the data for grain size distribution. For this sample the range of grain size variations (from 0.029 to 0.501 μm) is smaller than for others. Comparing the data for average grain size and variation of temperature during the process of decomposition of citrate precursor, one can conclude that the temperature and duration of the process of the precursor decomposition are the limiting factors to obtain the ferrite powders with smaller grain size. An optimum relation between

Table 1
Structural parameters of the $NiFe_2O_4$ samples obtained at various pH.

Composition	Space group	System	Lattice constant, a (Å)	Volume (Å^3)	Bragg R-factor
No. 1 (pH 2)	$Fd{-}3m$	Cubic	8.33749	579.570	2.09
No. 2 (pH 7)			8.33994	580.081	2.00
No. 3 (pH 11)			8.33924	579.934	2.80

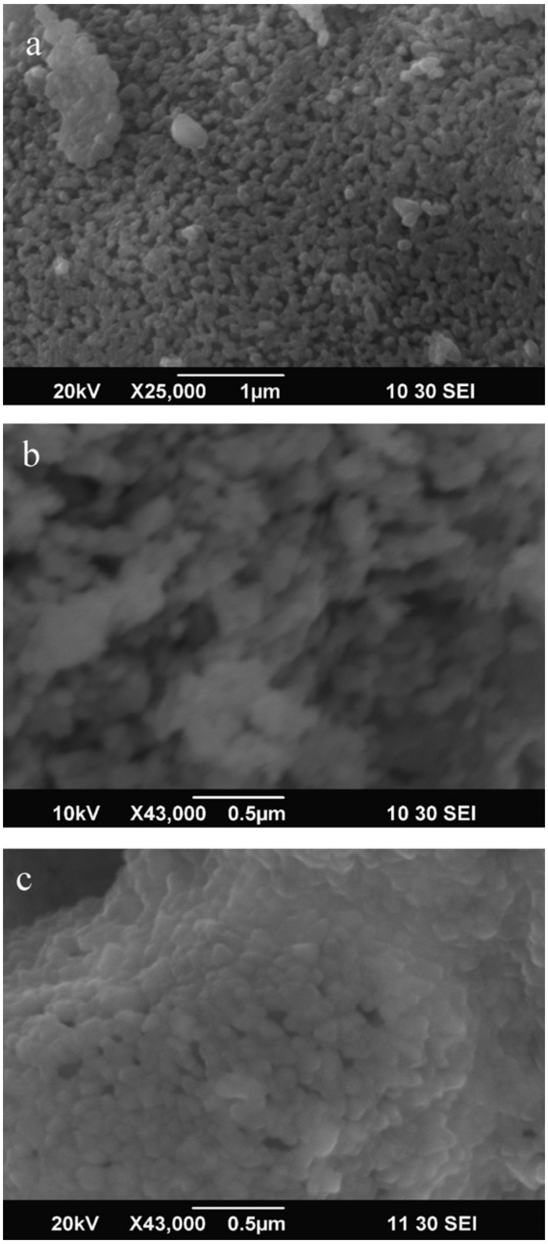

Fig. 5. SEM images of the surface of $NiFe_2O_4$ samples obtained by thermal decomposition of the citrate precursor with subsequent thermal treatment at temperature 900 °C: (a) for the sample No. 1 with pH 2, (b) for the sample No. 2 with pH 7, (c) for the sample No. 3 with pH 11.

the limiting factors can be determined experimentally by variation of pH.

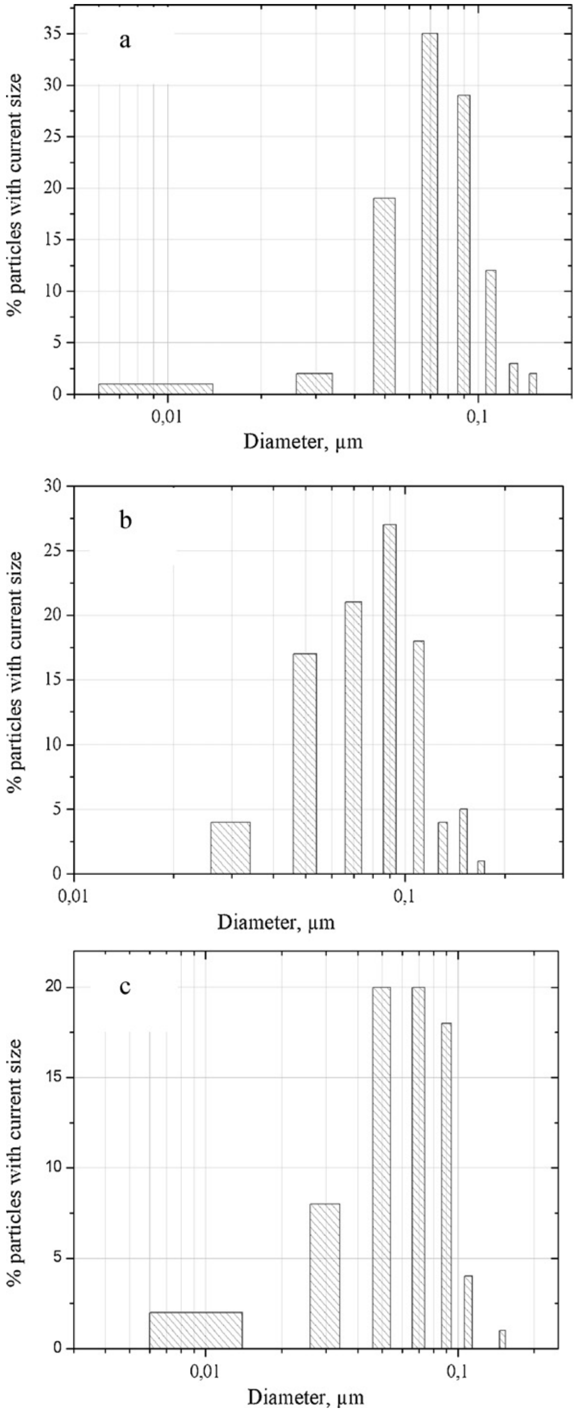

Fig. 6. Particle size distributions for the $NiFe_2O_4$ samples obtained by thermal decomposition of the citrate precursor with subsequent thermal treatment at temperature 900 °C: (a) for the sample No. 1 with pH 2, (b) for the sample No. 2 with pH 7, (c) for the sample No. 3 with pH 11.

For the samples under investigation static magnetic hysteresis loops were recorded both at 300 K and at 10 K. The results are shown in Fig. 7. Table 3 shows the magnetic characteristics (coercive force H_c, remnant magnetization σ_r, and saturation magnetization σ_s) obtained from the recorded hysteresis loops. As one can see from Fig. 7(a) and Table 3 for the sample No. 1 with pH 2 the magnetization curves at 300 K show very small hysteresis with $H_c = 64.5$ Oe, $\sigma_r = 17.63$ emu/g and $\sigma_s = 43.60$ emu/g, while at 10 K the finite coercivity of 294.2 Oe and comparable values of σ_r and σ_s are observed. For

Table 2
Statistical data for an average grain size of the polycrystalline $NiFe_2O_4$ samples determined from SEM images.

Composition	Average grain size (µm)	Absolute error (µm)	Ratio error (%)
No. 1 (pH 2)	0.079	0.0023	2.91
No. 2 (pH 7)	0.085	0.0029	3.41
No. 3 (pH 11)	0.066	0.0030	4.54

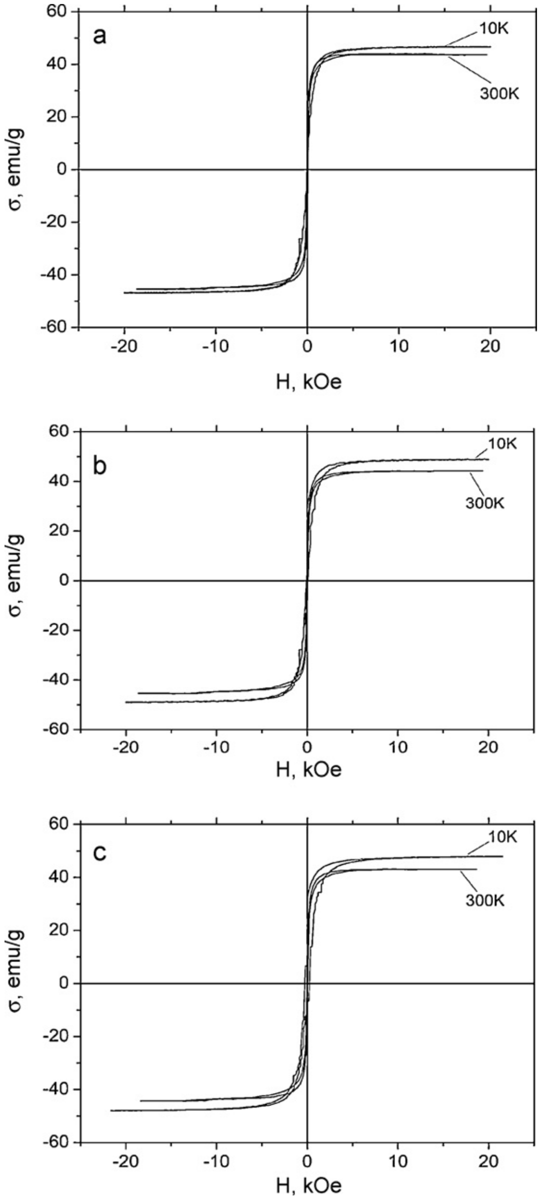

Fig. 7. Magnetization isotherms recorded at 300 K and 10 K for the $NiFe_2O_4$ samples obtained by thermal decomposition of the citrate precursor with subsequent thermal treatment at temperature 900 °C: (a) for the sample No. 1 with pH 2, (b) for the sample No. 2 with pH 7, (c) for the sample No. 3 with pH 11.

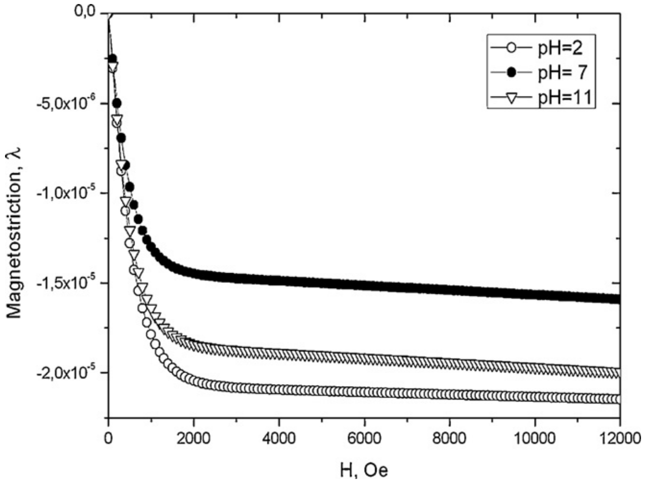

Fig. 8. Magnetostriction isotherms recorded at room temperature for the $NiFe_2O_4$ samples obtained by thermal decomposition of the citrate precursor with subsequent thermal treatment at temperature 900 °C.

this sample the ratio of σ_s(300 K)/σ_s(10 K) has the highest value of 0.93, as compared to the samples obtained at higher pH. With an account for higher values of σ_r both at 300 K and at 10 K, one can conclude that this sample is more magnetically homogeneous. The values of H_c at 300 K for all samples are rather close, however, they are much higher than the values for bulk polycrystalline $NiFe_2O_4$. This fact is in accordance with the available literature data [21]. The value of H_c at 10 K for the sample No. 3 with pH 11 is about 1.85 times larger than the corresponding value for the sample No. 1 with pH 2, which can be considered as another argument in favor of the better magnetic homogeneity of the sample with the lowest pH. The data for σ_r obtained are in good agreement with the corresponding values for nanodisperse particles obtained by various methods [22,23]. However, for the bulk samples of the same composition the values of σ_r are much higher [24]. Such decrease of residual magnetization with lowering the particle size can be explained by substantially larger specific area of polycrystalline powders and, as the consequence, appearance of a noncollinear spin structure originated from the pinning of the surface spins, which can be explained by the core–shell model of the nanoparticles consisting of ferrimagnetically aligned core spins and a spin glass-like surface layer. Thus the values of magnetic characteristics depend not only on the technological parameters, including the synthesis method, thermal treatment conditions, but also on the particle size.

Fig. 8 shows the magnetostriction isotherms obtained at room temperature. The values of saturation magnetostriction λ_s and magnetic field sensitivity of magnetostriction $d\lambda/dH$ are given in Table 4. As one can see, the value of λ_s is greatest for the sample No. 1, for which it is equal to -20.84×10^{-6}, while for two other samples the value of $\lambda_s = -18.78 \times 10^{-6}$ was obtained. In [25] for the polycrystalline $NiFe_2O_4$ samples obtained by solid state reactions method at temperatures 1000–

Table 3
Parameters of magnetic hysteresis loops recorded at 10 K and at 300 K.

Composition	H_c (Oe)		σ_r (emu/g)		σ_s (emu/g)	
	10 K	300 K	10 K	300 K	10 K	300 K
No. 1 (pH 2)	294.2	64.5	20.04	17.63	46.65	43.60
No. 2 (pH 7)	375.0	58.0	21.77	14.36	48.53	44.27
No. 3 (pH 11)	543.4	55.6	23.12	13.02	47.98	43.08

Table 4
Parameters of magnetostriction isotherms for $NiFe_2O_4$.

Composition	λ_s	$d\lambda/dH$ (Oe^{-1})
No. 1 (pH 2)	-20.84×10^{-6}	3.05×10^{-8}
No. 2 (pH 7)	-18.78×10^{-6}	2.51×10^{-8}
No. 3 (pH 11)	-18.78×10^{-6}	2.93×10^{-8}

1100 °C the λ_s value was found to be -26×10^{-6}. Such difference can be ascribed to the decrease of the particle size. For possible applications of magnetostrictive materials the magnetic field sensitivity of magnetostriction $d\lambda/dH$ is of prior importance. The value of $d\lambda/dH$ is maximum for the sample No. 1 and equals to 3.05×10^{-8} Oe^{-1}. The range of variation of the particle size is minimum for this sample.

The bulk samples obtained from powder No. 1 synthesized at pH 2 are characterized by optimum combination of magnetic and magnetostrictive properties: saturation magnetization $\sigma_s = 43.6$ emu/g, squareness of hysteresis loop $\sigma_r/\sigma_s = 0.4$, coercive force $H_c = 64.5$ Oe, saturation magnetostriction $\lambda_s = -20.84 \times 10^{-6}$, and sensitivity of magnetostriction to magnetic field $d\lambda/dH = 3.05 \times 10^{-8}$ Oe^{-1}.

4. Conclusions

In summary, the method of thermal decomposition of citrate precursor with subsequent thermal treatment has been used to obtain the ultra- and nanodisperse powders of spinel ferrite $NiFe_2O_4$. We show that variation of the composition of zole medium by the addition of ammonium hydroxide substantially influences the temperature conditions of decomposition of citrate precursors which, in turns, influences the final size distribution of spinel powders. The $NiFe_2O_4$ powders synthesized by this method have the cubic structure (space group $Fd{-}3m$) and are characterized by grain size distribution from 0.005 to 0.150 μm. An average grain size is minimum for the sample obtained at pH 11 and is equal to 0.066 μm. The temperature and duration of the process of precursor decomposition are limiting factors for decrease of the grain size. The optimum combination of the limiting factors can be experimentally adjusted by variation of pH. For the bulk samples obtained from powders synthesized at pH 2 optimum combination of magnetic and magnetostrictive properties was found.

Acknowledgements

This work was supported by the Russian Foundation for Basic Research (Grant No. 08-02-99062_r_ofi), Program of the fundamental research of the Presidium of RAS No. 21, Project of joint research of Ural and Siberian Branches of RAS No. 09-S-2-1016, Program of the Department of physical sciences of RAS ‘‘Spin phenomena in solid-state structures and spintronics’’.

References

[1] I.C. Nlebedim, N. Ranvah, P.I. Williams, Y. Melikhov, J.E. Snyder, A.J. Moses, D.C. Jiles, Effect of heat treatment on the magnetic and magnetoelastic properties of cobalt ferrite, J. Magn. Magn. Mater. 322 (14) (2010) 1929–1933.

[2] G. Schmid, Nanoparticles: From Theory to Application, New York, Wiley Interscience, 2004.

[3] A. Bardhan, C.K. Ghosh, M.K. Mitra, G.C. Das, S. Mukherjee, K.K. Chattopadhyay, Low temperature synthesis of zinc ferrite nanoparticles, Solid State Sci. 12 (5) (2010) 839–844.

[4] R.M. Mohamed, M.M. Rashad, F.A. Haraz, W. Sigmund, Structure and magnetic properties of nanocrystalline cobalt ferrite powders synthesized using organic acid precursor method, J. Magn. Magn. Mater. 322 (14) (2010) 2058–2064.

[5] K. Maaz, A. Mumtaz, S.K. Hasanain, A. Ceylan, Synthesis and magnetic properties of cobalt ferrite ($CoFe_2O_4$) nanoparticles prepared by wet chemical route, J. Magn. Magn. Mater. 308 (2) (2007) 289–295.

[6] X.-M. Liu, S.-Y. Fu, L.-P. Zhu, High-yield synthesis and characterization of monodisperse sub-microsized $CoFe_2O_4$ octahedra, J. Solid State Chem. 180 (2) (2007) 461–466.

[7] Y. Cheng, Y. Zheng, Y. Wang, F. Bao, Y. Qin, Synthesis and magnetic properties of nickel ferrite nano-octahedra, J. Solid State Chem. 178 (7) (2005) 2394–2397.

[8] P. Lavela, J.L. Tirado, $CoFe_2O_4$ and $NiFe_2O_4$ synthesized by sol–gel procedures for their use as anode materials for Li ion batteries, J. Power Sources 172 (1) (2007) 379–387.

[9] M. Georgea, A.M. Johna, Swapna S. Naira, P.A. Joyb, M.R. Anantharaman, Finite size effects on the structural and magnetic properties of sol–gel synthesized $NiFe_2O_4$ powders, J. Magn. Magn. Mater. 302 (1) (2006) 190–195.

[10] A. Baykal, N. Kasapoglu, Y. Koseoglu, M.S. Toprak, H. Bayrakdar, CTAB-assisted hydrothermal synthesis of $NiFe_2O_4$ and its magnetic characterization, J. Alloys Compd. 464 (2) (2008) 514–518.

[11] C. Yao, Z. Yuanhui, W. Yuansheng, B. Feng, Q. Yong, Synthesis and magnetic properties of nickel ferrite nano-octahedra, J. Solid State Chem. 178 (7) (2005) 2394–2397.

[12] B. Baruwati, S.V. Manorama, Monodispersed $NiFe_2O_4$ nanoparticles: nonaqueous synthesis and characterization, Mater. Chem. Phys. 112 (2) (2008) 631–636.

[13] S. Vivekanandhan, M. Venkateswarlu1, N. Satyanarayana, Effect of ethylene glycol on polyacrylic acid based combustion process for the synthesis of nano-crystalline nickel ferrite ($NiFe_2O_4$), Mater. Lett. 58 (22) (2004) 2717–2720.

[14] M. Salavati-Niasari, F. Davar, T. Mahmoudi, A simple route to synthesize nanocrystalline nickel ferrite ($NiFe_2O_4$) in the presence of octanoic acid as a surfactant, Polyhedron 28 (8) (2009) 1455–1458.

[15] N.S. Gajbhiye, S. Prasad, Thermal decomposition of hexahydrated nickel iron citrate, Thermochim. Acta 285 (2) (1996) 325.

[16] V.K. Sankaranarayanan, N.S. Gajbhiye, Thermal decomposition of dysprosium iron citrate, Thermohim. Acta 153 (1) (1989) 337.

[17] V.K. Sankaranarayanan, N.S. Gajbhiye, Low-temperature preparation of ultrafine rare-earth iron garnets, J. Am. Ceram. Soc. 73 (5) (1990) 1301–1307.

[18] K.S. Gavrilenko, T.V. Mironyuk, V.G. Il'in, S.N. Orlik, V.V. Pavlishchuk, From heteronuclear complex to a composite oxide. Approach in the synthesis of nanosized ferrites $M^{II}Fe2^{III}O4$ (M = Mn, Co, Ni) with spinel structure and their catalytic properties, Theor. Exp. Chem. 38 (2) (2002) 119–124.

[19] C-Y. Zhang, X.-Q. Shen, J.-X. Zhou, M.-X. Jing, K. Cao, Preparation of spinel ferrite $NiFe_2O_4$ fibres by organic gel-thermal decomposition process, J. Sol–Gel. Sci. Technol. 42 (1) (2007) 95–100.

[20] P. Gibart, G. Suran, AIP Conf. Proc. 29 (1975) 578 SpringerMaterials – The Landolt-Börnstein Database http://www.springermaterials.com.

[21] R.K. Mishra, G. Thomas, AIP Conf. Proc. 34 (1976) 66 SpringerMaterials – The Landolt-Börnstein Database http://www.springermaterials.com.

[22] S.G. Doh, E.B. Kim, B.H. Lee, J.H. Oh, Characteristics and synthesis of Cu–Ni ferrite nanopowders by coprecipitation method with ultrasound irradiation, J. Magn. Magn. Mater. 272–276 (3) (2004) 2238–2240.

[23] X.M. Liu, G. Yang, S.Y. Fu, Mass synthesis of nanocrystalline spinel ferrites by a polymer-pyrolysis route, Mater. Sci. Eng., C, Biomim. Mater., Sens. Syst. 27 (4) (2007) 750–755.

[24] R.H. Kodama, A.E. Berkowitz, E.J. Mcniff, S. Foner, Surface spin disorder in $NiFe_2O_4$ nanoparticles, Phys. Rev. Lett. 77 (2) (1996) 394–397.

[25] D.P. Raychaudhuri, Indian J. Phys. 9 (1935) 383 SpringerMaterials – The Landolt-Börnstein Database http://www.springermaterials.com.